

Phonon scattering studies of Ni and V centres in GaP and InP

This article has been downloaded from IOPscience. Please scroll down to see the full text article.

1989 J. Phys.: Condens. Matter 1 9313

(<http://iopscience.iop.org/0953-8984/1/47/004>)

View [the table of contents for this issue](#), or go to the [journal homepage](#) for more

Download details:

IP Address: 171.66.16.96

The article was downloaded on 10/05/2010 at 21:05

Please note that [terms and conditions apply](#).

Phonon scattering studies of Ni and V centres in GaP and InP

M Sahraoui-Tahar†, B Salce‡, L J Challis†, N Butler†, W Ulrici§ and B Cockayne||

† Department of Physics, University of Nottingham, Nottingham NG7 2RD, UK

‡ Centre d'Etudes Nucleaires, Service des Basses Temperatures, 85X, 38041 Grenoble Cédex, France

§ Akademie der Wissenschaften der DDR, Berlin, Zentralinstitut für Elektronphysik, 1086 Berlin, German Democratic Republic

|| Royal Signals and Radar Establishment, St Andrews Road, Great Malvern, Worcs WR14 3PS, UK

Received 26 June 1989

Abstract. Thermal conductivity measurements have been made from 50 mK to 100 K of GaP and InP samples doped with Ni or V. The GaP samples both show strong resonant phonon scattering at 500 and 380 GHz respectively which is attributed to the T_1 – T_2 tunnelling splitting associated with a dynamic orthorhombic Jahn–Teller distortion of the T_1 orbital ground state of Ni^{2+} and V^{2+} . Low-frequency scattering in both systems is tentatively attributed to these same ions in complex with a defect. The assignment of the scattering to V^{2+} is supported by studies of photo-induced changes in the V^{2+} concentration. Uniaxial stress measurements on GaP:V suggest strong coupling to E modes but the strength of the coupling to T_2 modes is less clear. The absence of resonance scattering in a n-type sample of InP:Ni suggests the Ni is all in the Ni^+ state (2T_2) as expected and the absence of scattering in n-type InP:V is consistent with the instability of V^{2+} in that system.

1. Introduction

Thermal conductivity studies of the Cr^{3+} ($3d^3$) ion in GaAs, GaP and InP (Challis *et al* 1982, Ramdane *et al* 1983, Butler *et al* 1985, 1986) show that it is very strongly coupled to phonons. The high-spin ground state given by Hund's rule is 4T_1 and the strong sensitivity of the energy levels to both $\langle 100 \rangle$ (E) and $\langle 111 \rangle$ (T_2) uniaxial stress indicates that, unusually, the Jahn–Teller distortion for this system is orthorhombic with potential wells lying along the six $\langle 110 \rangle$ directions. This confirmed the results of an earlier investigation of EPR under uniaxial stress on Cr^{3+} in GaAs (Krebs and Stauss 1977, Stauss and Krebs 1980). If the electron–lattice interaction is weak or modest then the Hamiltonian describing the potential energy of the coupled system is 'linear' and this leads to minima along the $\langle 100 \rangle$ and $\langle 111 \rangle$ directions and a saddle point along the $\langle 110 \rangle$ direction. The resulting Jahn–Teller distortions are either tetragonal or trigonal depending on which minimum lies lowest. The orthorhombic behaviour is believed to be the result of very strong electron–lattice coupling which leads to large Jahn–Teller distortions and hence to significant non-linear terms in the Hamiltonian. These terms eventually convert the

$\langle 110 \rangle$ saddle points into minima so that there can now be potential minima along the $\langle 100 \rangle$, $\langle 111 \rangle$ and $\langle 110 \rangle$ directions and, if the coupling is strong enough, the $\langle 110 \rangle$ minima can lie lowest leading to orthorhombic behaviour, though not to orthorhombic symmetry since the dynamic terms restore this to T_d . The six orbital eigen-states associated with the $\langle 110 \rangle$ minima form the representation $T_1 + T_2$ and tunnelling between them splits the two triplets (Muramatsu and Iida 1970, Bersuker and Polinger 1974, Sakamoto 1982, Lister and O'Brien 1984, Bates *et al* 1987). This splitting gives rise to strong resonant phonon scattering at the frequency corresponding to the triplet separation. The spin-orbit splitting of the two triplets should be strongly quenched by the Jahn–Teller effect so that little or no fine structure is to be expected in this resonance.

The behaviour exhibited by Cr^{3+} is actually much more complicated than this. Its sensitivity to both E and T_2 strains is consistent with the orthorhombic model as already noted and this, together with the strong scattering observed in zero stress, is inconsistent with a strongly coupled tetragonal or trigonal Jahn–Teller distortion. (This is discussed further by Challis *et al* 1989.) However, the system showed resonant scattering at several frequencies and not just one as predicted by the orthorhombic model. Recently, these studies of T_1 ground-state systems were extended to Ni^{2+} ($3d^8$) in GaAs (Challis *et al* 1989) and this 3T_1 system appears to be consistent with the model in every major respect. Not only are the energy levels sensitive to both E and T_2 stress but, in this case, the resonant scattering is limited to a single frequency of 300 ± 30 GHz. The stress dependence indicates that the coupling constants are appreciably weaker than in Cr^{3+} and the authors suggest that in Cr^{3+} ion–ion coupling via the strain field is responsible for additional splittings and so for additional resonant scattering. There has also been an investigation of a third system V^{2+} ($3d^3$) in GaAs which should again have a 4T_1 ground state in the high-spin case and so, by analogy, be expected to show similar properties; it is in fact isoelectronic with Cr^{3+} . However, in this case no resonant scattering due to V^{2+} ions could be detected in the frequency range above 100 GHz and although scattering was seen at much lower frequencies, 6 and 20 GHz, changes in the strength of this produced by low-temperature optical illumination decayed very much more slowly than other properties associated with V^{2+} , suggesting that this low-frequency scattering could not be due to isolated V^{2+} (Butler *et al* 1987, 1989a, Sahraoui-Tahar *et al* 1989). It is in fact attributed to a V^{2+} complex also seen in thermally detected EPR (En-Naqadi *et al* 1988) and acoustic paramagnetic resonance (Rampton *et al* 1986). It is suggested that this very different behaviour of V^{2+} from that expected for a 4T_1 ground state indicates that it adopts the low-spin 2E ground state, as recently predicted theoretically (Katayama-Yoshida and Zunger 1986, Caldas *et al* 1986). Further experimental evidence supporting this has recently been published by Görger *et al* (1988).

In the present investigation we have extended these studies of T_1 ground states to Ni^{2+} and V^{2+} in GaP and InP. Ni enters readily into substitutional sites in GaP and has been observed in three valence states, Ni^{3+} ($3d^7$), Ni^{2+} ($3d^8$) and Ni^+ ($3d^9$) (Clerjaud 1985 and references therein). Ni^{3+} should have an orbital ground state (4A_2) and so only scatter phonons very weakly and Ni^+ (2T_2), by analogy with Cr^{2+} (5T_2), should be expected to undergo a tetragonal Jahn–Teller effect and scatter phonons at very low frequencies only: < 5 GHz in the case of Cr^{2+} in GaAs (Challis *et al* 1982), corresponding to the tunnelling frequency between the wells. Less appears to be known about Ni in InP: Ni^+ has recently been detected optically and the $\text{Ni}^+/\text{Ni}^{2+}$ level shown to be at $E_c - 0.27$ eV (Korona *et al* 1989). Ni^{3+} has been observed by EPR (Kaufmann and Schneider 1978) and Clerjaud also notes three other investigations. Ni in association with a defect may also be present in these systems, although no additional phonon

scattering at low frequencies. (~ 10 GHz) attributable to a Ni^{2+} complex was seen in GaAs:Ni (Challis *et al* 1989). V enters into substitutional sites in GaP and InP and a number of optical investigations have been made on both systems (Ulrici *et al* 1987, 1989a, Ulrici and Kreissl 1988, Devaud *et al* 1986 and references therein). In GaP it appears that three valence states can exist: V^{2+} ($3d^3$) which should have a ${}^4\text{T}_1$ ground state, V^{3+} ($3d^2$) which should have an orbital singlet ground state (${}^3\text{A}_2$), and V^{4+} ($3d^1$) which should have a ${}^2\text{E}$ ground state. In InP it appears that only V^{4+} and V^{3+} can exist since the $\text{V}^{2+}/\text{V}^{3+}$ level lies in the conduction band (Devaud *et al* 1986). Neither V^{3+} nor V^{4+} should scatter phonons strongly so that, at the concentrations present, any detectable scattering above 1 K in GaP is likely to be from V^{2+} and none is expected in InP. We note also that resonant scattering at low frequencies (6 and 20 GHz) in GaAs:V is attributed to a V^{2+} complex (Butler *et al* 1989a) so that the possibility exists of similar scattering below 1 K in the present systems.

2. Experimental details

Measurements of thermal conductivity were made in the temperature range 50 mK to 100 K covering the phonon frequency range 5–1000 GHz. Standard techniques were used and the absolute values of conductivity are accurate to $<15\%$, the principal error being in the determination of the separation of the two thermometer contacts (typically 10 ± 1 mm). The data are presented both as thermal conductivity K plotted against temperature and also as W/W_0 against temperature where W ($=1/K$) and W_0 are, respectively, the thermal resistivities of the doped sample and a pure sample. For GaP there are in fact no experimental conductivity data for samples of sufficient purity. The purity requirement is particularly demanding for a semiconductor with an indirect gap since this leads to structure in the ground state of any shallow donors present and so to strong resonant phonon scattering in the frequency range of interest. Hence the values of W_0 for GaP were calculated from theoretical fits to the experimental data for doped samples as described below.

Measurements of thermal conductivity on the GaP sample after illumination with sub-band gap radiation were made above 1 K using a monochromator and fibre-optic system and below 1 K using an infrared diode emitting a broad-band spectrum covering the photon energy range 1–2 eV. Measurements under compressive uniaxial stress were carried out using the technique used by Ramdane *et al* (1983) and described by Salce (1984).

3. Experimental results

3.1. GaP:Ni

A $\langle 110 \rangle$ axis sample (Ela) of cross section 2.76×2.82 mm² was cut from LEC-grown material prepared at the Zentralinstitut für Elektronenphysik, Berlin. It has high resistivity and is p-type at room temperature. Optical absorption and EPR measurements (Ulrici *et al* 1989b) show that the material contains both Ni^{2+} and Ni^{3+} , indicating that the Fermi level is pinned by the $\text{Ni}^{2+}/\text{Ni}^{3+}$ level at $E_v + 0.51$ eV and so is very unlikely to contain any Ni^+ in the dark since the $\text{Ni}^+/\text{Ni}^{2+}$ level is nearly 1 eV higher (these level

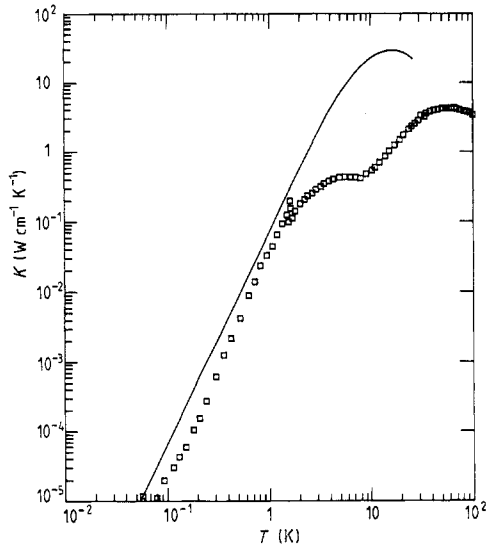


Figure 1. The thermal conductivity of GaP:Ni. The full curve shows the conductivity K_0 calculated for pure GaP.

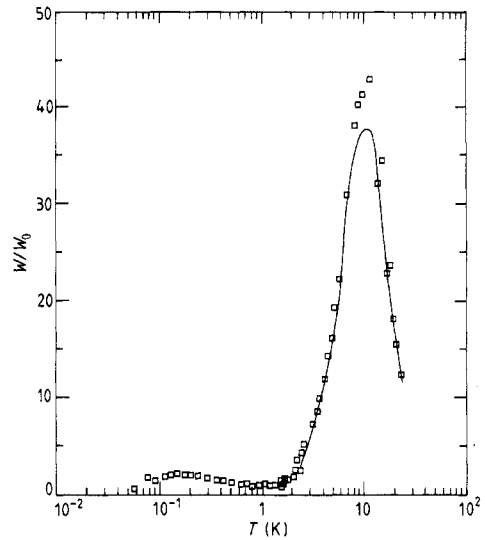


Figure 2. The reduced thermal resistivity W/W_0 of GaP:Ni. The full curve is a theoretical fit to the data above 1 K. The resonance at 10 K is attributed to Ni^{2+} and that at 0.15 K to a Ni^{2+} complex.

positions are given by Clerjaud 1985). The thermal conductivity is shown in figure 1. Resonant scattering is apparent from the dips around 10 K and 0.15 K. This is seen more clearly in the plot of W/W_0 shown in figure 2. (The values are higher than those given by Butler *et al* 1989b who used values of W_0 scaled from GaAs.) A theoretical description of the conductivity data above 1 K was obtained by assuming $\tau^{-1} = \nu/L + A\omega^4 + B\omega_n^2 T^3 + C\omega^4/(\omega^2 - \omega_0^2)^2$ and adjusting the various parameters to get the best fit which is shown by the full curve. The first three terms describe boundary scattering, point-defect scattering and phonon-phonon scattering respectively, and the last term is the resonant scattering rate characteristic of the elastic process that should be dominant at these frequencies. W_0 was then calculated by omitting the resonant term but retaining the point-defect term; K_0 is shown as a full curve in figure 1. The resonant frequency $\nu_0 = \omega_0/2\pi = 500 \pm 50$ GHz is assumed to be the $T_1 - T_2$ splitting and the value of C is $4.0 \times 10^8 \text{ s}^{-1}$. We have not attempted to fit the data below 1 K but the temperature of the maximum suggests a resonant scattering frequency around 12 GHz ($h\nu_0 = 3.8 kT$). This frequency is similar to those seen in GaAs:V and, by analogy, we suggest that it is due to a Ni^{2+} complex with a 3T_1 ground state.

3.2. GaP:V

Four GaP:V samples were cut from LEC material grown in Berlin. Two samples A1 and E1 (A = seed end, E = tail) were cut from one boule and PI1535A1 and PI1535E1 from another which was co-doped with Zn. Sample E1 is semi-insulating and has a cross section of $3.19 \times 3.38 \text{ mm}^2$, and A1 is weakly p-type ($p \sim 5 \times 10^{16} \text{ cm}^{-3}$ at room temperature) with cross section $2.92 \times 3.01 \text{ mm}^2$. PI1535A1 and PI1535E1 are both p-type ($p \sim 4 \times 10^{15} \text{ cm}^{-3}$ and $7 \times 10^{16} \text{ cm}^{-3}$ at room temperature, respectively) and have cross sections of $2.94 \times 3.03 \text{ mm}^2$ and $2.97 \times 3.02 \text{ mm}^2$ respectively. Sample A1 has a (112)

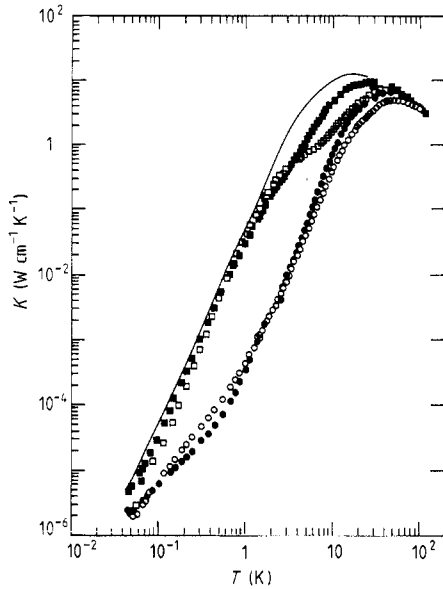


Figure 3. The thermal conductivity of GaP:V. \square , El(si); \blacksquare , Al (p-type); \bullet , PI1535Al (p-type); \circ , PI1535E1 (p-type). The full curve shows the conductivity K_0 calculated for pure GaP.

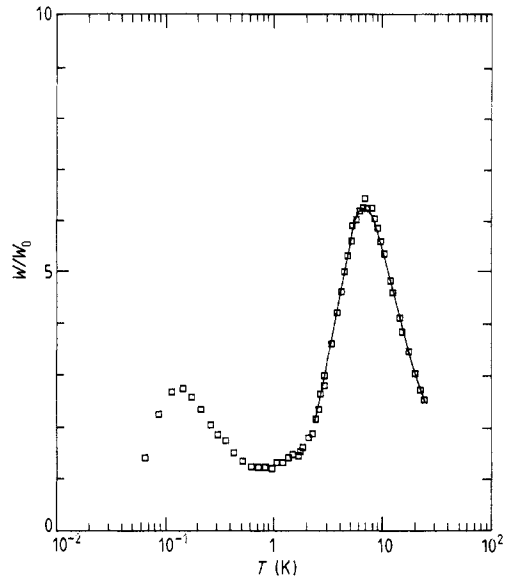


Figure 4. The reduced thermal resistivity W/W_0 of si GaP:V (El). The full curve is a theoretical fit to the data above 1 K. The resonance at 7 K is attributed to V^{2+} and that at 0.15 K to a V^{2+} complex.

axis and the other three have $\langle 110 \rangle$ axes. Optical and EPR measurements on the same boules by Ulrici *et al* (1987) show that the semi-insulating (si) sample El contains V^{2+} and V^{3+} while Al only contains V^{4+} . SIMS analysis on El shows that its total V concentration is $4 \times 10^{16} \text{ cm}^{-3}$. The thermal conductivities are shown in figure 3 and compared with the K_0 values obtained from the GaP:Ni data. The data for the p-type sample PI1535Al are somewhat lower near the peak than those calculated for pure GaP but show no evidence of resonant scattering. This agrees with evidence from optical studies showing that at low temperatures the Fermi level is pinned at the V^{3+}/V^{4+} level (Ulrici *et al* 1989a) so that the sample contains neither V^{2+} nor neutral acceptors, both of which would scatter phonons. The data for El (si) and Al and PI1535E1 (p-type) are plotted as W/W_0 in figures 4 and 5 using the calculated values for W_0 obtained from El. The corresponding values of K_0 are shown in figure 3. They are somewhat smaller near the peak than those in figure 1 as a larger point-defect term was needed in the fit to El.

The resonant scattering in the si sample El (figure 4) is seen to be very similar in form to that for GaP:Ni (figure 2). A fit to the data above 1 K was obtained as before and indicates a resonant frequency of $\nu_0 = \omega_0/2\pi$ of 380 ± 40 GHz, somewhat lower than that for Ni^{2+} as can be deduced from the temperatures of the two peaks. The value of C is $2.6 \times 10^7 \text{ s}^{-1}$. The frequency of the process responsible for the low-frequency peak is estimated to be 12 GHz ($h\nu_0 = 3.8 kT$).

The large values of W/W_0 for the two p-type samples (Al and PI1535E1) are attributed to phonon scattering from neutral acceptors. The Γ_8 ground state of the bound hole should scatter phonons strongly in this frequency range with a peak near to $q \sim 1/a_0^*$, where a_0^* is the Bohr radius and q the phonon wavenumber, as has been shown in other systems (see e.g., Challis and de Goër 1984; the peak in the scattering may in fact be

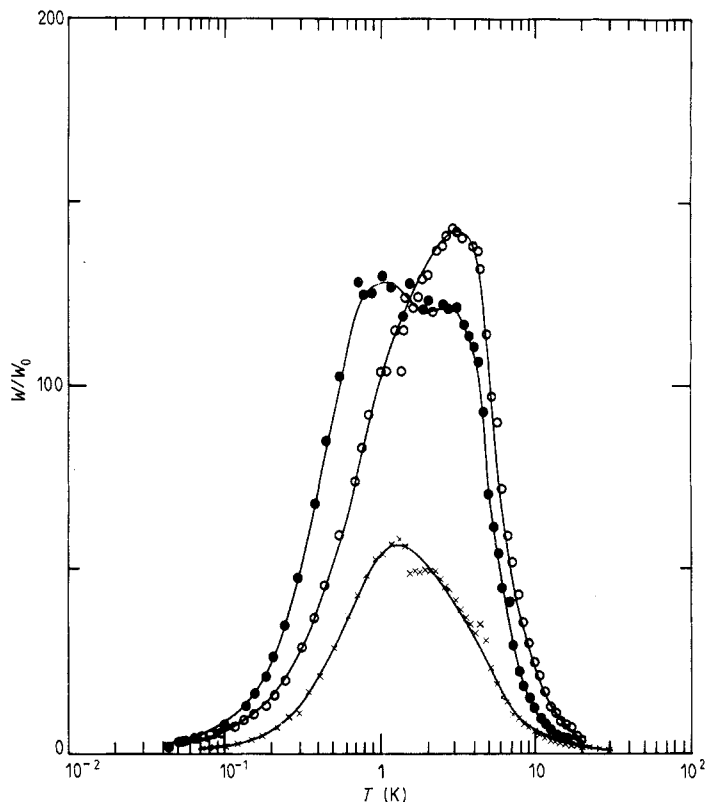


Figure 5. The reduced thermal resistivity W/W_0 of p-type GaP:V: \circ , (PI1535El); \bullet , Al. Also shown (\times) is the reduced thermal resistivity of a p-type sample of GaAs:V:Zn (CT806). The curves are to guide the eye.

shifted to lower frequencies by resonant scattering associated with a Jahn–Teller effect within the Γ_8 ; see Sigmund 1984). The W/W_0 data for PI1535El containing Zn acceptors has a single peak and may be compared with those for a GaAs:V:Zn sample, CT806 (Butler *et al* 1989a), which shows similar behaviour (figure 5). The frequencies corresponding to $q = 1/a_0^*$ in the two systems are ~ 650 (GaP) and ~ 270 GHz (GaAs) which are indeed larger, by a factor of ~ 2.5 , than those deduced from the temperatures of the peaks assuming $h\nu_0 = 3.8 kT$: 250 (GaP) and 100 GHz (GaAs) (we take $a_0^* = 1$ nm, $v = 4.1 \times 10^3$ m s $^{-1}$ (GaP) and $a_0^* = 2$ nm, $v = 3.3 \times 10^3$ m s $^{-1}$ (GaAs)). W/W_0 for Al appears to have two peaks suggesting that the scattering is from two different neutral acceptors. Low temperature illumination from the diode produced no measurable effect on the resistivity below 1 K of either sample and the measurements were not extended above.

We next investigated the effects of sub-band-gap radiation on the semi-insulating sample (El). No effects were seen on the conductivity below 1 K but pronounced effects were seen above. These were made by illuminating the sample at 6 K with radiation from a monochromator. The photon energy was increased in steps from just above the cut-off E_{co} of the optical fibre at 0.8 eV, until an increase occurred in the thermal resistivity. The energy was then held fixed and the illumination continued until the increase saturated. The energy was then increased a small amount and the process

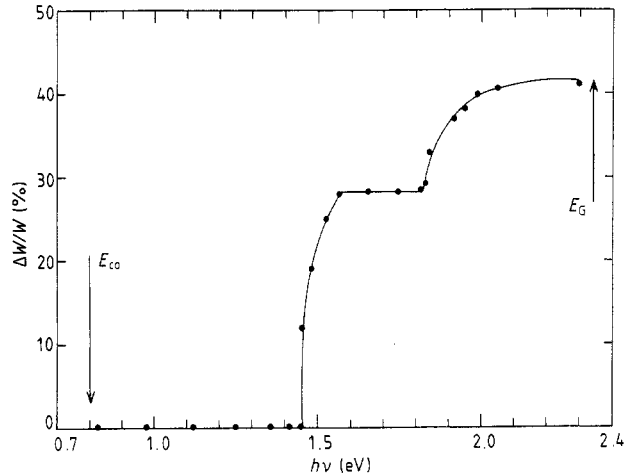


Figure 6. Changes, $\Delta W/W$, in the thermal resistivity of GaP:V (EI) attributed to the photoproduction of V^{2+} . W is the resistivity before illumination. E_{co} shows the cut-off in the optical fibre and E_G the energy gap.

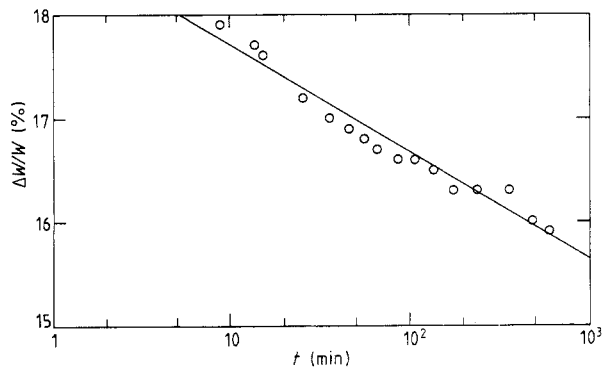


Figure 7. The decay at 6 K of the additional thermal resistivity $\Delta W/W$ created by optical illumination of GaP:V (EI). W is the resistivity before illumination.

repeated until the band-gap energy E_G was reached. The results are shown in figure 6; there are clear onsets at 1.45 and 1.82 eV. The spectral dependence of this photo-induced increase in thermal resistivity is almost identical to the spectral dependence of the photo-induced increase of V^{2+} measured by optical absorption (Ulrici *et al* 1987). We have also examined the decay of the additional resistivity $\Delta W/W$ following illumination at 1.56 eV while the sample was at 6 K and the results are shown in figure 7 (small corrections have been made to allow for drift). The decay is logarithmic with time as is the photo-induced absorption (Ulrici and Kreissl 1988), though the resistivity decays more slowly.†

† In a preliminary interpretation, it was suggested that the decay required the presence of two scattering centres (Butler *et al* 1989b). We note too that the timescale in figure 2(b) of that paper should read 1×10^4 , 2×10^4 , etc, and that the additional resistivity is rather larger than that shown.

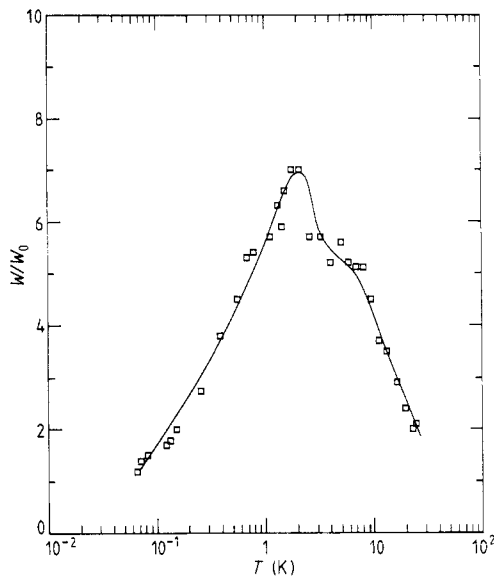


Figure 8. The reduced thermal resistivity W/W_0 of the p-type sample PI1535Al after illumination. The curve is to guide the eye.

It seems clear that the additional scattering produced by optical illumination is due to V^{2+} which must therefore scatter phonons strongly in this range of frequencies. It seems reasonable to infer that the scattering seen above 1 K before illumination is also due to V^{2+} and that the resonant frequency of 380 GHz corresponds to the tunnelling splitting ($T_1 - T_2$) associated with a 4T_1 high-spin ground state. It is less clear, however, whether the low-frequency phonon scattering can be assigned to a V complex of some sort as might be expected by analogy with GaAs : V. TDEPR experiments on the SI material EI do show a V^{2+} spectrum, very similar to that seen in GaAs, but it only appears after optical illumination (Vasson and Vasson 1989) while the 12 GHz phonon scattering is present in the dark and is unaffected by illumination. So this might suggest they are not from the same centre. Another complication is that the spectral dependence of the TDEPR spectrum is identical to that found for isolated V^{2+} in optical absorption and in phonon scattering above 1 K (figure 6).

Further work is evidently needed to clarify the situation and establish the centre(s) responsible for these low-frequency effects. Additional evidence of these valence changes was obtained by illuminating the p-type sample PI1535Al at 4 K with light from the infrared diode. The effect of illumination with light of $h\nu > 1.3$ eV is known from optical and EPR measurements to result in a recharging process via a phosphorus antisite leading to $V^{3+} \rightarrow V^{4+} + \text{hole}$ (Ulrici *et al* 1989a). Hole capture by acceptors will then lead to the formation of neutral acceptors which will act as phonon scatterers. The results in figure 8 seem consistent with this. The main peak is presumably due to Zn acceptors and the shoulder perhaps apparent on the high-temperature side may be due to other neutral acceptors, although we cannot rule out the possibility that it is V^{2+} created by the illumination since that would not be seen in the optical and EPR work. All illumination effects could be annealed out by warming the sample to room temperature.

Measurements were also made on the semi-insulating sample EI as a function of uniaxial stress using $\langle 100 \rangle$ and $\langle 111 \rangle$ axis samples and applying compressive stress along the axes as previously described; the results are shown in figure 9. Both samples broke at stresses of about 1700 kgf cm^{-2} and measurements have only been made at 1.9 K

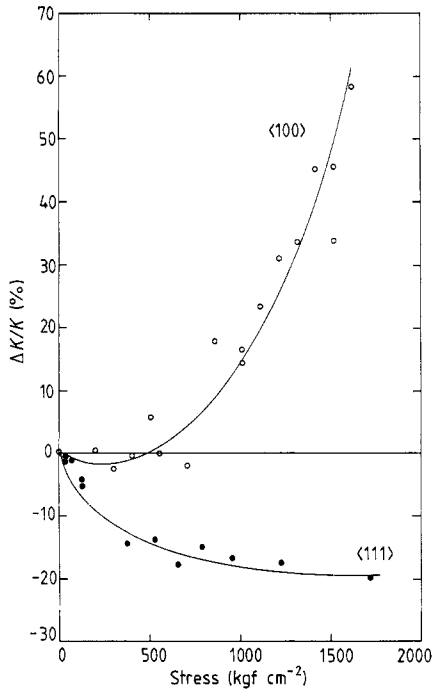


Figure 9. The change in thermal conductivity of sr GaP: V (EI) produced by $\langle 100 \rangle$ and $\langle 111 \rangle$ uniaxial stress.

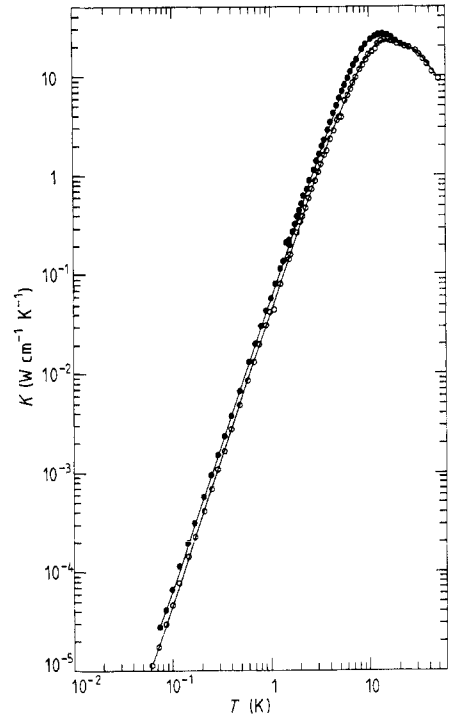


Figure 10. The thermal conductivity of n-type samples of: \circ , InP: Ni; \bullet , InP: V.

where the thermal resistivity is about 60% larger than that estimated for pure GaP (figure 4). This implies that for $\langle 100 \rangle$ stress of 1700 kgf cm^{-2} the conductivity must be close to its saturation value and it has a value of half this at a stress of around 1400 kgf cm^{-2} . This is similar to the stress producing the same relative effect in the conductivity of Ni^{2+} in GaAs (Challis *et al* 1989) suggesting that their values of the electron–lattice coupling constant V_{Eb} are also similar. We conclude that for V^{2+} in GaP, $V_{Eb} = 40\,000 \pm 15\,000 \text{ cm}^{-1}$. The steady reduction in conductivity produced by $\langle 111 \rangle$ stress is very different however from the rise seen in Ni^{2+} in GaAs and the fall to a minimum at $50\text{--}100 \text{ kgf cm}^{-2}$ (2 K) seen for Cr^{3+} in GaAs, GaP and InP. It is possible that the $\langle 111 \rangle$ data in figure 9 will reach a minimum at 2000 kgf cm^{-2} and that this implies that V_{Tb} is less by a factor $2000/(50 \rightarrow 100)$ than in Cr^{3+} . However, it seems more likely that the fall in conductivity is the result of crack formation in the sample preceding its breakage.

3.3. InP: Ni

The $\langle 111 \rangle$ axis sample L1062 of dimensions $1.04 \times 1.05 \times 11 \text{ mm}^3$ was cut from LEC-grown material from RSRE. The Ni concentration determined by SIMS was below the detection limit of $1 \times 10^{16} \text{ cm}^{-3}$. However, in a neighbouring sample, the Ni was found to be inhomogeneously distributed with a concentration $> 5 \times 10^{16} \text{ cm}^{-3}$ so it seems probable that the concentration in L1062 must be close to $1 \times 10^{16} \text{ cm}^{-3}$. It is n-type at room temperature so the Ni should all be in the Ni^+ state (2T_2). The thermal conductivity

between 50 mK and 100 K is shown in figure 10 and it is seen that there is no evidence of resonant scattering in the whole range. As noted earlier, $\text{Ni}^+(\text{}^2\text{T}_2)$, by analogy with Cr^{2+} in GaAs, might be expected to undergo a tetragonal Jahn–Teller effect and scatter phonons at the tunnelling frequency. For Cr^{2+} , this occurs at <5 GHz (Challis *et al* 1982) and the tail of the resonant scattering is seen as an increase in W/W_0 below 100 mK. The absence of a similar increase at temperatures down to 50 mK could suggest that the tunnelling frequency in Ni^+ in InP is less than half that of Cr^{2+} in GaAs (assuming Ni^+ distorts as suggested). However, as was pointed out previously for Ni^+ in GaAs (Challis *et al* 1989), which also produces no detectable low-frequency scattering, we cannot totally rule out the possibility that the tunnelling frequency occurs at similar frequencies to Cr^{2+} but the scattering is quenched by random strains. Measurements were also made below 1 K after optical illumination with the diode but no effects were seen and they were not extended above 1 K. No photoluminescence could be detected in this material (Skolnick 1989) which is consistent with recent observations by Korona *et al* (1989) showing that the Ni^+ excited level lies in the conduction band.

3.4. InP:V

The $\langle 111 \rangle$ axis sample L1022 of dimensions $1.05 \times 1.05 \times 7 \text{ mm}^3$ was cut from LEC material grown at RSRE and is n-type at room temperature. The V concentration measured by spark source mass spectroscopy is approximately $2 \times 10^{16} \text{ cm}^{-3}$ and the photoluminescence spectrum seen is attributed to V^{3+} (Skolnick *et al* 1983). The thermal conductivity between 50 mK and 100 K is shown in figure 10 and again shows no evidence of resonant scattering in this range. This is consistent with evidence that V^{2+} does not exist in InP: n-type material should only contain V^{3+} ions which are weak phonon scattering centres. The absence of scattering below 1 K might suggest that there is no stable V^{2+} complex in InP similar to that in GaAs.

4. Discussion

The observation in GaP samples of resonant scattering at 500 and 380 GHz attributable to Ni^{2+} and V^{2+} respectively seems wholly consistent with the presence of orthorhombic Jahn–Teller effects acting on a T_1 orbital ground state. The levels of the V^{2+} ion are sensitive to E strains but the coupling to T_2 strains is less clear since the $\langle 111 \rangle$ stress dependence may be masked by the effects of stress-induced damage to the sample. It would be of interest to repeat and extend these data and to have similar data for Ni^{2+} in GaP but the fragility of GaP results in a rather low success rate. Orthorhombic Jahn–Teller effects have also been identified previously in Ni^{2+} in GaAs and in Cr^{3+} in GaAs, GaP and InP though in these three latter systems the observations are complicated by what is now thought to be ion–ion coupling through the strain field.

We conclude that the data for all six of the T_1 systems we have investigated are consistent with orthorhombic Jahn–Teller distortions and this raises questions as to why these particular systems should all be so strongly coupled and whether this is a general property of all T_1 systems in T_d sites. Figure 4 of Lister and O'Brien (1984) shows that the orthorhombic case occupies a third of the parameter space but, since the systems are more strongly coupled to E modes than to T_2 modes, we are usually only concerned with the left-hand side of the figure. For the present systems, the parameter measuring the

strength of the non-linear terms must evidently be positive taking them into the top left-hand quarter of the figure where there is an orthorhombic region, and since the ratio of E to T_2 mode coupling cannot be very large it is reasonable that they should lie within it. These conditions could well apply to a large number of the strongly coupled T_1 systems so that perhaps the most interesting question now is whether all T_1 systems are very strongly coupled to the lattice in T_d symmetry and if so why.

The fact that the lattice coupling in T_d sites is much stronger to T_1 ground-state ions than to E is readily associated with the positions of the ligands with respect to the e and t_2 lobes of the electronic wavefunctions as, of course, is the greater crystal-field energy of the t_2 orbitals. This does not however explain why T_1 ions (V^{2+} , Cr^{3+} , Ni^{2+}) should apparently be much more strongly coupled than T_2 ions (Cr^{2+} , Ni^{+}) and we suggest that the reason for this lies not in their difference in symmetry, but in the fact that the T_1 ions all come from d^3 or d^8 configurations while the T_2 ions come from d^4 or d^9 . The d^3 and d^8 configurations are rarely found as compounds in T_d symmetry because of the higher destabilising energy in this coordination and it seems reasonable to suppose therefore that, when they are in T_d symmetry as impurities, their energy levels will be very sensitive to distortions which lower the symmetry.

A final point of interest is the fact that V^{2+} in GaP obeys Hund's rule and has a 4T_1 ground state while V^{2+} in GaAs does not and presumably has a 2E low-spin ground state. This is in disagreement with the theoretical analysis by Caldas *et al* (1986) which predicted that both should adopt the low-spin case and may imply that the energies of the two states 2E and 4T_1 lie very close to each other in both systems so that their order is difficult to calculate.

Acknowledgments

We are very grateful to Mr W R McEwan for help preparing samples, Mr D Arnaud, Mr J-A Favre, Mr J-M Martinod, Mr W B Roys and Dr M S Skolnick for their help, Drs A-M and A Vasson for allowing us to refer to their recent unpublished results and Professor C A Bates, Dr B Clerjaud and Dr M C M O'Brien for valuable discussions. We are particularly grateful to Dr O'Brien for pointing out why the orthorhombic case may be rather widespread and for discussions on the coupling to T_1 ions. We are also grateful to the Science and Engineering Research Council and the Royal Society for financial support, and to the SERC for the award of a research fellowship (NB), and the Algerian Ministry of Higher Education for Scientific Research and the British Council for the award of a research studentship (M S-T).

References

- Bates C A, Dunn J L and Sigmund E 1987 *J. Phys. C: Solid State Phys.* **20** 1965–83
 Bersuker I B and Polinger V Z 1974 *Zh. Eksp. Teor. Fiz.* **66** 2078–91 (Engl. Trans. 1975 *Sov. Phys.-JETP* **39** 1023–9)
 Butler N, Jouglar J, Salce B, Challis L J and Vuillermoz P L 1985 *J. Phys. C: Solid State Phys.* **18** L725–30
 Butler N, Jouglar J, Salce B, Challis L J, Ramdane A and Vuillermoz P L 1986 *Proc. 5th Int. Conf. on Phonon Scattering in Condensed Matter, Urbana, IL, 1986* ed. A C Anderson and J P Wolfe (Berlin: Springer) pp 123–5
 Butler N, Challis L J, Sahraoui-Tahar M, Salce B and Ulrici W 1987 *Japan J. Appl. Phys.* **26** 675–6
 Butler N, Challis L J, Sahraoui-Tahar M, Salce B and Ulrici W 1989a *J. Phys. Condens. Matter* **1** 1191–203

- Butler N, Challis L J, Sahraoui-Tahar M, Salce B, Ulrici W and Cockayne B 1989b *Proc. 15th Int. Conf. Defects in Semiconductors (Budapest) 1988; Mat. Sci. Forum* **38–41** 905–10
- Caldas M J, Figueirido S K and Fizzio A 1986 *Phys. Rev. B* **33** 7102–9
- Challis L J and de Goër A-M 1984 *The Dynamical Jahn–Teller Effects in Localised Systems* ed. Yu Perlin and M Wagner (Amsterdam: North-Holland) pp 533–708
- Challis L J, Locatelli M, Ramdane A and Salce B J 1982 *J. Phys. C: Solid State Phys.* **15** 1419–32
- Challis L J, Salce B, Butler N, Sahraoui-Tahar M and Ulrici W *J. Phys.: Condens. Matter* **7** 7277–93
- Clerjaud B 1985 *J. Phys. C: Solid State Phys.* **18** 3615–6
- Devaud B, Plot B, Lambert B, Bremond G, Guillot G, Nouailhat A, Clerjaud B and Naud C 1986 *J. Appl. Phys.* **59** 3126–30
- En-Naqadi M, Vasson A, Vasson A-M, Bates C A and Labadz A F 1988 *J. Phys. C: Solid State Phys.* **21** 1137–53
- Görger A, Meyer B K, Spaeth J-M and Hennel A M 1988 *Semiconductor Sci. Technol.* **3** 832–8
- Katayama-Yoshida H and Zunger A 1986 *Phys. Rev. B* **33** 2961–4
- Kaufmann U and Schneider J 1978 *Solid State Commun.* **25** 1113–6
- Korona K, Hennel A M and Baranowski J M 1989 *Acta Phys. Polon. A* **75** 151–3
- Krebs J J and Stauss G H 1977 *Phys. Rev. B* **15** 17–22
- Lister G M S and O'Brien M C M 1984 *J. Phys. C: Solid State Phys.* **17** 3975–86
- Muramatsu S and Iida T 1970 *J. Phys. Chem. Solids* **31** 2209–16
- Ramdane A, Salce B and Challis L J 1983 *Phys. Rev. B* **27** 2554–7
- Rampton V W, Saker M K and Ulrici W J 1986 *J. Phys. C: Solid State Phys.* **19** 1037–43
- Sahraoui-Tahar M, Butler N, Challis L J, Salce B and Ulrici W 1989 *Proc. 19th Int. Conf. on Physics of Semiconductors, Warsaw, 1988* ed. W Zawadzki (Warsaw: Polish Academy of Sciences) pp 1019–22
- Sakamoto N 1982 *Phys. Rev. B* **26** 6438–43
- Salce B 1984 *Proc. 4th Int. Conf. Phonon Scattering in Condensed Matter, Stuttgart, 1983* ed. W Eisenmenger, K Lassmann and S Dottinger (Berlin: Springer) pp 58–60
- Sigmund E 1984 *The Dynamical Jahn–Teller Effects in Localised Systems* ed. Yu Perlin and M Wagner (Amsterdam: North-Holland) pp 495–532
- Skolnick M S 1989 private communication
- Skolnick M S, Dean P J, Kane M J, Uihlein C H, Robbins D J, Hayes W, Cockayne B and MacEwan W R 1983 *J. Phys. C: Solid State Phys.* **16** L767–75
- Stauss G H and Krebs J L 1980 *Phys. Rev. B* **22** 2050–9
- Ulrici W, Eaves L, Friedland K and Halliday D P 1987 *Phys. Status Solidi b* **141** 191–202
- Ulrici W and Kreissl J 1988 *Proc. 5th Int. Conf. Semi-insulating III–V Materials, Malmo, 1988* ed. G Grossmann and L Lebedo (Bristol: Adam Hilger) pp 381–6
- Ulrici W, Kreissl J, Hayes D G, Eaves L and Friedland K 1989a *Proc. 15th Int. Conf. Defects in Semiconductors (Budapest) 1988; Mater. Sci. Forum* **38–41** 875–80
- Ulrici W et al 1989b private communication
- Vasson A-M and Vasson A 1989 private communication
- Vasson A-M, Vasson A, Bates C A and Labadz A F 1984 *J. Phys. C: Solid State Phys. C* **17** L837–41